JOURNAL OF Materials CHEMISTRY

Merocyanine dyes: dimeric aggregation in solution, film structure and pH sensing

Geoffrey J. Ashwell,*[a] Karl Skjonnemand,[a] Gary A. N. Paxton,[a] David W. Allen,[b] Joanne P. L. Mifflin[b] and Xing Li[b]

[a]*The Nanomaterials Group, Centre for Photonics and Optical Engineering, The Whittle Building, Cranfield University, Cranfield, UK MK43 0AL. E-mail: g.j.ashwell@cranfield.ac.uk*
[b]*Division of Chemistry, Sheffield Hallam University, Sheffield, UK SW1 1WB*

Received 12th December 2000, Accepted 7th February 2001
First published as an Advance Article on the web 20th March 2001

4-(*N*-Hexadecylquinolinium-4-ylmethylideneamino)-2,6-dichlorophenolate (**1a**) aggregates in low polarity solvents with an equilibrium constant for dimerisation and Gibbs free energy of $K = 4500 \pm 700\ M^{-1}$ and $\Delta G^{\circ} = -20.5 \pm 0.4\ kJ\ mol^{-1}$ respectively in chloroform at 20 °C. The aggregating molecules probably adopt an antiparallel arrangement in solution but, nonetheless, form non-centrosymmetric Langmuir–Blodgett (LB) structures. The films are purple with $\lambda_{max} = 580$ nm but, in an acidic environment, reversibly change to yellow with $\lambda_{max} = 410$ nm. The real and imaginary components of the relative permittivity at 632.8 nm are $\varepsilon_r = 3.0$ and $\varepsilon_i = 1.0$ (merocyanine dye) and $\varepsilon_r = 2.1$ and $\varepsilon_i = 0.0$ (protonated form), these data corresponding to a refractive index change of $\Delta n \approx 0.3$. Consequently, the films may be used as the active component of a surface plasmon resonance device to detect either ammonia or acidic gases at ppm concentrations. The properties are compared with those of the pyridinium analogue, 4-(*N*-hexadecylpyridinium-4-ylmethylideneamino)-2,6-dichlorophenolate (**2a**) as well as the dibromo analogues of each. The four dyes form dimeric solution aggregates.

Introduction

LB films of amphiphilic donor–(π-bridge)–acceptor materials have been extensively studied for second-harmonic generation (SHG)[1,2] and some of the more polar examples have been found to adopt an antiparallel arrangement both in solution[3] and within the monolayer.[4] The alignment may be controlled by lengthening the hydrophobic tail and this has been found to

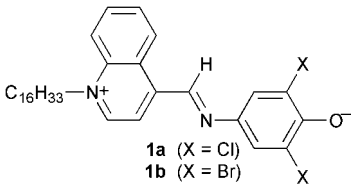

1a (X = Cl)
1b (X = Br)

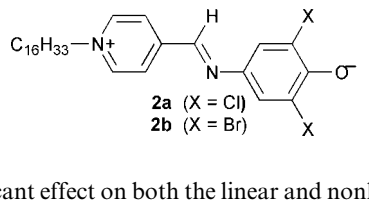

2a (X = Cl)
2b (X = Br)

have a significant effect on both the linear and nonlinear optical behaviour. For example, the zwitterionic dye, [(*Z*)-β-(*N*-alkyl-4-quinolinium)-α-cyano-4-styryl]dicyanomethanide, R-Q3CNQ, which acts as a molecular rectifier[5,6] as well as an optically nonlinear material,[4,7] forms purple LB films with a high second-order susceptibility of $\chi_{zzz}^{(2)} = 180\ pm\ V^{-1}$ at 1.064 μm when $R \geqslant C_{16}H_{33}$ but its films are turquoise and effectively SHG-inactive when $R \leqslant C_{14}H_{29}$. The transition reflects an altered alignment,[4] from H-type (parallel) to J-type (antiparallel), with van der Waals interactions between the hydrophobic tails and intermolecular charge-transfer contributing to the stability of the former and latter respectively. The molecules have a large ground-state dipole moment of 43 ± 8 D, aggregate in less polar solvents and exhibit negative solvatochromism.[7,8] These are common features of zwitterionic materials and Würthner and Yao[3] have reported the occurrence of dimeric solution aggregates from the concentration dependence of the dipole moment of some related dyes. They have suggested that the molecules adopt a centric antiparallel arrangement.

The merocyanine dyes reported in this work also form dimeric aggregates in solution and, like many other derivatives,[9–13] exhibit significant negative solvatochromism. We report their deposition by the LB technique and characterisation by surface plasmon resonance (SPR), atomic force microscopy (AFM) and quartz crystal microbalance (QCM) studies. The dyes readily protonate, both at the air–water interface and in air, and may be used to sense ammonia at ppm concentrations by monitoring changes in the normalised reflectance from glass–Au–monolayer structures.

Experimental

Synthesis

Solvents and reagents were obtained from the Aldrich Chemical Company and reactions were carried out under an atmosphere of nitrogen. The synthesis of the pyridinium analogues has been reported elsewhere.[14]

4-(*N*-Quinolin-4-ylmethylideneamino)-2,6-dichlorophenol. A solution of 4-amino-2,6-dichlorophenol (1.43 g, 8 mmol) and quinoline-4-carbaldehyde (1.26 g, 8 mmol) in ethanol (20 cm^3) was heated at reflux for three hours. The reaction mixture was cooled and the precipitate washed with ethanol to afford yellow–green crystals of the imine: yield 2.42 g (95%); mp 261–

DOI: 10.1039/b009914g

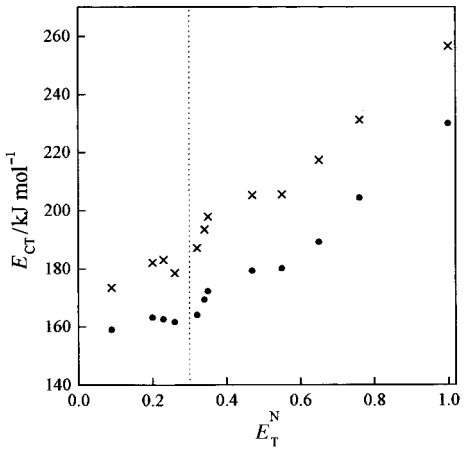

Fig. 1 Variation of the energy of the intramolecular charge-transfer band of **1** (●) and **2** (×) with Reichardt's normalised solvent polarity parameter: toluene ($E^N_T = 0.09$), tetrahydrofuran (0.20), ethyl acetate (0.23), chloroform (0.26), dichloromethane (0.32), benzonitrile (0.34), acetone (0.35), acetonitrile (0.47), propan-2-ol (0.55), ethanol (0.65), methanol (0.76) and water (1.00). Both dyes are insoluble in water and thus, the data at $E^N_T = 1.00$ relate to their *N*-methyl analogues. The chloro and bromo derivatives exhibit identical spectra and aggregate with multiple maxima in solvents to the left of the vertical line but have a single charge-transfer band in those to the right.

263 °C. δ_H (TFA): 7.32 (s, 2H, Ar–H); 8.04–8.40 (m, 6H, Ar–H and CH=N); 9.08–9.22 (dd, 1H, Ar–H); 10.65 (s, 1H, OH). HRMS (EI), *m/z*: calcd. for $C_{16}H_{10}N_2{}^{35}Cl_2O$, 316.0170; found 316.0164 (M^+).

4-(*N*-Quinolin-4-ylmethylideneamino)-2,6-dibromophenol. The dibromo derivative was obtained from 4-amino-2,6-dibromophenol using the procedure described above: yellow–green crystals; yield 83%; mp 248–249 °C. δ_H (TFA): 7.56 (s, 2H, Ar–H); 8.11–8.46 (m, 6H, Ar–H and CH=N); 9.17–9.28 (dd, 1H, Ar–H); 10.71 (s, 1H, OH). HRMS (EI), *m/z:* calcd. for $C_{16}H_{10}N_2{}^{79}Br^{81}BrO$, 405.9139; found: 405.9149 (M^+).

4-(*N*-Hexadecylquinolinium-4-ylmethylideneamino)-2,6-dichlorophenolate (1a). An anhydrous DMF solution (30 cm^3) of the imine, 4-(*N*-quinolin-4–ylmethylideneamino)-2,6-dichlorophenol (1 g, 3.2 mmol), 1-iodohexadecane (1.13 g, 3.2 mmol) and silver toluene-*p*-sulfonate (0.89 g, 3.2 mmol) was stirred for three days in the dark at 80–100 °C. The solution was filtered to remove AgI. The filtrate was poured into aqueous KI and extracted with dichloromethane (4×100 cm^3). The combined organic layers were washed with water, dried ($MgSO_4$) and the solvent evaporated *in vacuo* to leave a green–black solid (0.26 g). The crude product was purified by column chromatography on silica gel eluting initially with dichloromethane–methanol (5 : 95, v/v) and then methanol to give **1a** as blue–black crystals: yield 0.1 g (6%); mp 114–120 °C (decomp.). δ_H ($CDCl_3$): 0.88 (t, 3H, CH_3); 1.24–1.67 (br m, 24H, CH_2); 1.89 (m, 2H, CH_2); 3.65 (m, 2H, CH_2); 4.92 (t, 2H, CH_2N^+); 7.12 (s, 2H, Ar–H); 7.53–8.10 (m, 5H, Ar–H); 8.74 (s, 1H, CH=N); 8.92 (d, 1H, Ar–H). HRMS (FAB), *m/z*: calcd. for $C_{32}H_{43}N_2{}^{35}Cl_2O$, 541.2752; found 541.2738 $(M+H)^+$.

4-(*N*-Hexadecylquinolinium-4-ylmethylideneamino)-2,6-dibromophenolate (1b). By analogy with the preparation of **1a**, the dibromo derivative was obtained from 4-(*N*-quinolin-4-ylmethylideneamino)-2,6-dibromophenol using the procedure described above: blue–black crystals; yield 6%; mp 158–160 °C. δ_H ($CDCl_3$): 0.86 (t, 3H, CH_3); 1.13–1.24 (br m, 24H, CH_2); 1.98–2.30 (m, 2H, CH_2); 3.60 (m, 2H, CH_2); 4.77 (t, 2H, CH_2N^+); 7.34 (s, 2H, Ar–H); 7.34–7.97 (m, 5H, Ar–H); 8.56 (s, 1H, CH=N); 8.82 (d, H, Ar–H). HRMS (FAB), *m/z*: calcd. for $C_{32}H_{44}N_2{}^{79}Br^{81}BrO$, 632.1800; found 632.1796 $(M+2H)^+$.

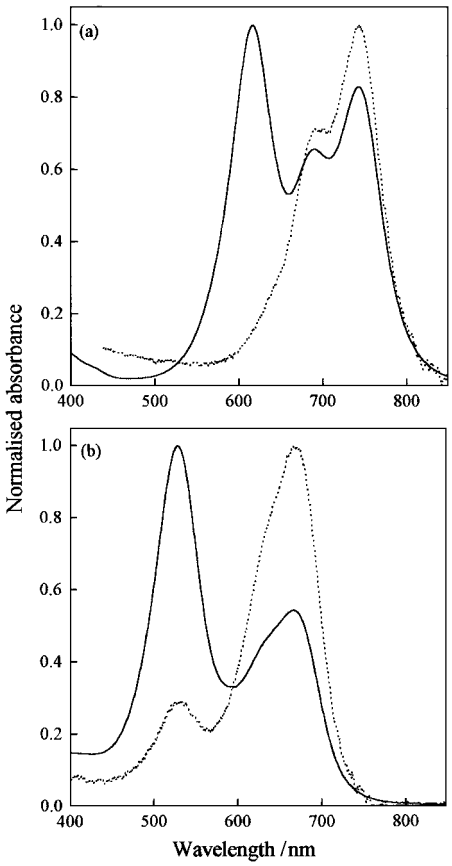

Fig. 2 Normalised spectra showing different behaviour in concentrated (solid line) and dilute (broken line) chloroform solutions: (a) dye **1**; (b) dye **2**. The bands at lower and higher wavelengths correspond to intermolecular and intramolecular transitions respectively.

Langmuir and LB films

The merocyanine dyes were spread from dilute chloroform solution (2×10^{-4} M) onto the pure water subphase of an LB trough (Nima Technology, model 622). They were left for 10 min at *ca.* 2 °C and then compressed at 0.5 cm^2 s^{-1} (*ca.* 0.1% s^{-1} of compartment area) to obtain pressure–area (π–A) isotherms. Surface potential studies were performed under identical conditions. Films were deposited on the upstroke by passing the following substrates through the floating monolayer at 30 μm s^{-1}: gold coated BK7 glass (for SPR studies), gold coated 10 MHz quartz crystals (QCM), silicon wafers (AFM), and hydrophilically treated glass slides (spectra). The monolayer thickness and contact area, from SPR and QCM studies respectively, were obtained for deposition pressures of 5 to 35 mN m^{-1} whereas the principal investigation was performed on films deposited at 15 mN m^{-1}.

Results and discussion

Solution studies

The dyes exhibit negative solvatochromism, *i.e.* a red shift of the visible absorption band as the solvent polarity decreases, this common feature of merocyanine derivatives being frequently attributed to a zwitterionic ground state.[9–13] However, contrary to this, Hamman and El-Nahas[15] have suggested that the hydrogen-bonding ability of the donor is a

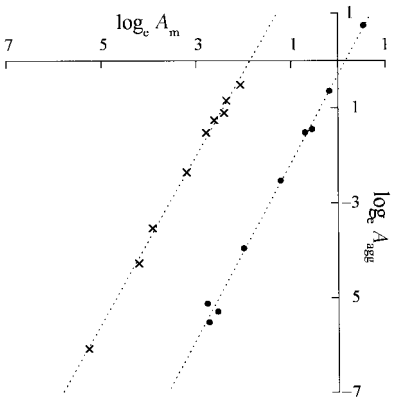

Fig. 3 Variation of $\log_e(A_{agg})$ with $\log_e(A_m)$ where A_{agg} and A_m correspond to absorbances of the aggregate and monomer in chloroform: **1** (●) and **2** (×). The aggregate absorbance of dye **1** has been corrected for the slight overlap of the neighbouring absorption band. The chloro and bromo analogues of each show indistinguishable behaviour.

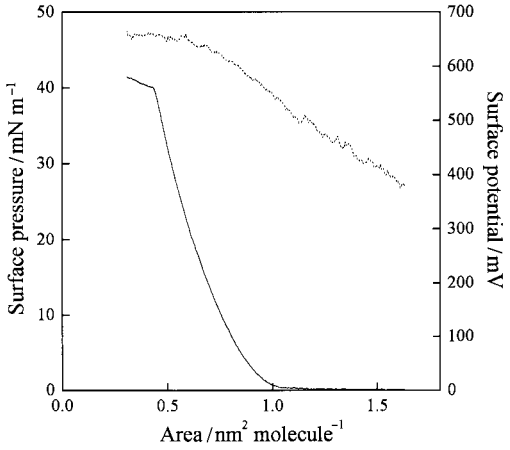

Fig. 4 Surface pressure *versus* area isotherm of **1a** (solid line) and variation of its surface potential with area (broken line). Areas were calculated using the molecular mass of the unprotonated form but the dye is partially protonated in air and thus, the actual area is larger than indicated. The bromo analogue shows similar behaviour.

vital factor and Alberti and Echave[16] have reported nucleophile–carbonyl interactions (*e.g.* in acetone) and hydrogen-bonding (*e.g.* in methanol) as the cause of the experimentally observed behaviour. Furthermore, Catalan *et al.*[17] have demonstrated that *tert*-butyl groups, *ortho* to the oxygen of the phenolate donor, significantly weaken the solvatochromism but, as above, the wavelength increases with decreasing solvent polarity. In this work, the solvent dependence of the low energy charge-transfer bands of **1** and **2** is shown in Fig. 1, the data being depicted as the transition energy *versus* Reichardt's normalised polarity parameter (E^N_T).[18] The spectra of the quinolinium and pyridinium analogues are independent of the halo substituent and, for each of the solvents, the transition energy of dye **1** is 26 ± 3 kJ mol^{-1} higher than **2** for $E^N_T > 0.3$. However, this is not necessarily valid for less polar solvents where aggregation influences the wavelengths of the charge-transfer bands. Consequently, there is slight deviation in the low E^N_T region.

The dyes each have a single symmetrical charge-transfer band when $E^N_T > 0.3$ but exhibit multiple maxima in less polar solvents. For example, the quinolinium analogue exhibits charge-transfer bands at *ca.* 610 nm, 690 (sh) and 740 nm when dissolved in chloroform and a peak absorbance ratio, $A_{740nm} : A_{610nm}$, that decreases with increasing concentration (Fig. 2a). This may be explained by aggregation whereby the high-energy band corresponds to the intermolecular transition of the aggregate and the low-energy band and its shoulder to intramolecular transitions of the monomer and aggregate respectively. The equilibrium constant is given by:

$$K = [\text{aggregate}]/[\text{monomer}]^n \quad (1)$$

where n is the association number and the concentration terms are proportional to absorbance, *i.e.* $c = A/\varepsilon_o l$ where ε_o and l are the molar absorption coefficient and pathlength respectively. The slope of $\log_e(A_{agg})$ *versus* $\log_e(A_m)$, corresponding to the absorbance of the aggregate and monomer at 610 and 740 nm respectively, provides an association number of $n \approx 2$ (Fig. 3). Such aggregation probably corresponds to an antiparallel coupling of the zwitterionic D–π–A chromophores and, from the report of Würthner and Yao[3] and charge-transfer spectra of other analogues,[7,8] appears to be a common feature of such dyes. The data yield an equilibrium constant for dimerisation and Gibbs free energy of $K = 4500 \pm 700$ M^{-1} and $\Delta G^\circ = -20.4 \pm 0.4$ kJ mol^{-1} respectively for **1a** in chloroform at 20 °C.

The pyridinium dyes (**2a** and **2b**), as for the quinolinium analogue above, are mainly unassociated in polar solvents but form dimeric aggregates in chloroform with maxima at *ca.* 525 and 670 nm (Fig. 2b). These correspond to the intermolecular and intramolecular transitions respectively and, in this case, the Benesi–Hildebrand[19] analysis yields an equilibrium constant of $K > 2 \times 10^6$ M^{-1} for **2a** (*cf.* 4500 M^{-1} for **1a**). Thus, the molecules are almost completely aggregated at concentrations used in the LB study. However, the dimeric aggregates need not affect the film structure because the molecules exist as monomers in polar solvents and an aqueous subphase ($E^N_T = 1$) is used for their deposition.

Floating monolayers

The surface pressure *versus* area (π–A) isotherms of the different halo derivatives are similar and, therefore, only the data for the chloro analogues are shown (Figs. 4 and 5). The quinolinium and pyridinium dyes have limiting areas of 0.45 and 0.35 nm^2 respectively, just prior to collapse, with the latter corresponding to the broadest molecular cross-section, *i.e.* the dichlorophenolate group. Thus, the chromophores are vertically aligned in the high-pressure regime and the antiparallel J-aggregated dimers, which exist in chloroform, clearly disintegrate when the dyes are spread on an aqueous subphase. They show no evidence of aggregation in polar solvents ($E^N_T > 0.3$)

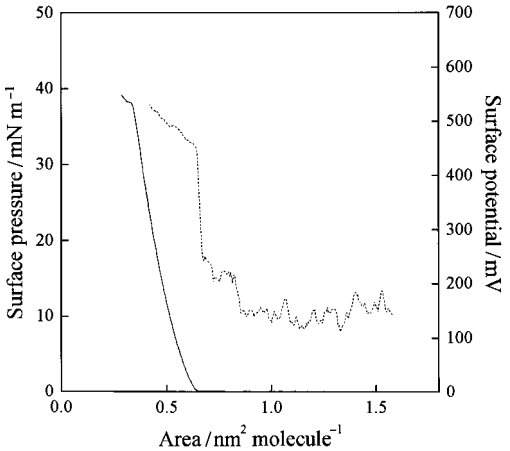

Fig. 5 Surface pressure *versus* area isotherm of **2a** (solid line) and variation of its surface potential with area (broken line). Areas were calculated using the molecular mass of the unprotonated form but the dye is partially protonated in air and thus, the actual area is larger than indicated. The bromo analogue shows similar behaviour.

at concentrations used in the LB study and we note that Reichardt's normalised polarity parameter for the subphase is unity.

The surface potential *versus* area data indicate that the two dyes behave differently at the air–water interface (Figs. 4 and 5) and, although not shown, results for the chloro and bromo analogues of each are similar to those of the parent dyes. The pyridinium analogues exhibit an abrupt step in potential, at *ca.* 0.68 nm^2 $molecule^{-1}$ for **2a**, which relates to the limiting area of the pressure–area isotherm at $\pi = 0$. In contrast, the quinolinium analogues exhibit significantly higher potentials that gradually rise as the pressure is increased. The induced potential results from an alignment of the molecular dipoles, perpendicular to the air–water interface, and to an increased dipole density upon compression. The non-polar alkyl groups have a slight effect due to changes in the dielectric thickness but more significant changes result from a vertical orientation of the zwitterionic chromophores. Therefore, the data of Fig. 4 suggest that **1a** is partially tilted prior to compression whereas those of Fig. 5 indicate that **2a** tilts abruptly upwards as the floating layer is compressed.

Deposited films

Preliminary accounts of the sensing properties of the two pyridinium analogues on conventional substrates[14] as well as optical fibres[20] have been reported and are excluded from this work. However, data from SPR studies are included for direct comparison with results obtained for films of the quinolinium analogue. Studies were performed on glass–Au–monolayer structures by attenuated total reflection using the Kretschmann geometry.[21] Analysis of the data gave a thickness of 2.2 ± 0.3 nm for monolayer films of **2a** deposited at $20 \leqslant \pi \leqslant 35$ mN m^{-1} but a spread of values for the real and imaginary parts of the relative permittivity: $\varepsilon_r = 2.1$ to 2.5 and

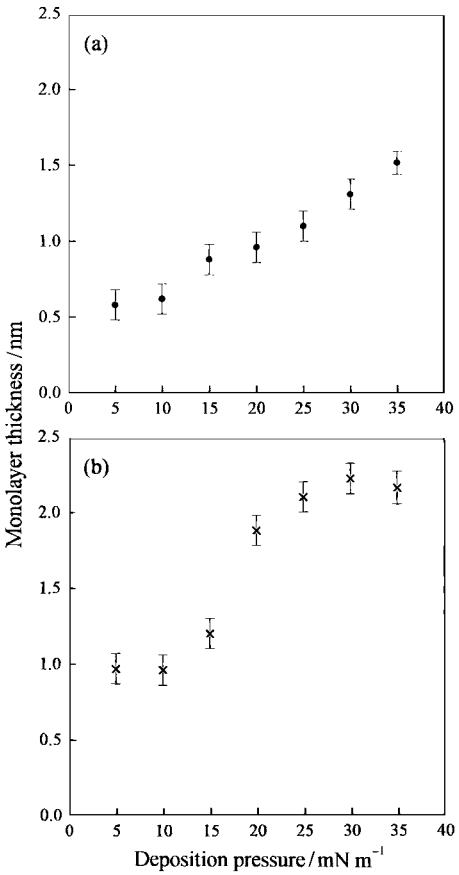

Fig. 6 Monolayer thickness *versus* deposition pressure: (a) dye **1a**; (b) dye **2a**.

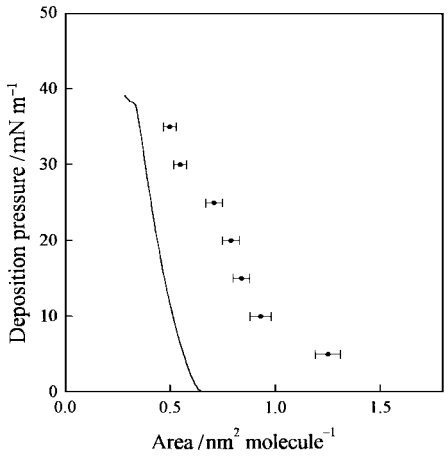

Fig. 7 Deposition pressure *versus* the area in contact with the central gold electrodes of the quartz crystal substrate, the data being obtained from QCM studies on monolayer films of **1a** and compared with the surface pressure *versus* area isotherm (solid line).

$\varepsilon_i = 0.0$ to 0.2 for $\lambda = 632.8$ nm. We have not previously observed such a wide variation and, while confident of the fitting routine, suggest that the experimental data are dependent upon the degree of protonation when deposited from a slightly acidic aqueous subphase. Differences arise from the fact the merocyanine films are purple with $\lambda_{max} = 510$ nm but, when protonated, change to a yellow with $\lambda_{max} = 375$ nm and cut-off above 550 nm. Furthermore, the films probably contain structural voids, which also affect the apparent relative permittivity, this being indicated by a large footprint area from QCM studies.

The quinolinium analogue (**1a**), which now forms the basis of this discussion, forms better quality films which exhibit weak SHG, indicative of non-centrosymmetric alignment, and whose dimensions are dependent upon the deposition pressure. The monolayer thickness shows a gradual increase from 0.6 to 1.5 nm as π alters from 5 to 35 mN m^{-1} (Fig. 6) and this is accompanied by a decrease in the molecular area, from 1.25 to 0.50 nm^2, in contact with the substrate (Fig. 7). The areas, obtained from a Sauerbrey analysis[22] of the QCM data, are significantly larger than those indicated by the isotherm, a feature reported for other dyes where X-ray analysis has confirmed an altered packing arrangement.[23] Furthermore, AFM images of films deposited at 15 mN m^{-1} exhibit a molecular footprint of 0.8 nm^2, consistent with the area obtained from the QCM data. They also show a series of

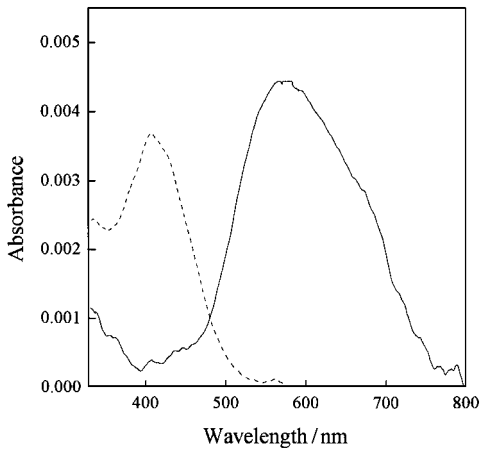

Fig. 8 Absorption spectra of a monolayer of **1a** deposited at 15 mN m^{-1}: merocyanine form (solid line) and protonated form (broken line).

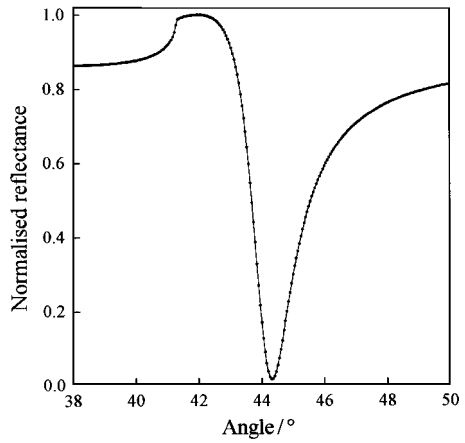

Fig. 9 SPR spectrum for a glass–Au–monolayer structure of the unprotonated form of **1a** deposited at 15 mN m^{-1} and obtained at $\lambda = 632.8$ nm. The theoretical line corresponds to the following: gold, $d = 50.66$ nm, $\varepsilon_r = -10.48$ and $\varepsilon_i = 1.34$; monolayer, $d = 1.09$ nm, $\varepsilon_r = 2.94$ and $\varepsilon_i = 0.93$. The resonant angle was shifted by $+0.02°$ when the film was exposed to ammonia resulting in $\varepsilon_r = 3.0$ and $\varepsilon_i = 1.0$.

parallel lines with a lattice spacing of 2.00 nm (*cf.* 3 nm molecular length), which suggest that the molecules are tilted towards the substrate. The volume, from the product of area and thickness, is constant at *ca.* 0.75 nm^3 molecule^{-1} for films deposited at $5 \leqslant \pi \leqslant 35$ mN m^{-1} and provides a density of 1.2 Mg m^{-3}.

The LB films are readily affected by protonation and change from purple ($\lambda_{max} = 580$ nm) to yellow ($\lambda_{max} = 410$ nm), with the latter being transparent above 580 nm (Fig. 8). Such changes are also reflected by SPR, the resonant angle being shifted to higher values when the LB film is exposed to ammonia and to lower values when exposed to acid. As for the pyridinium analogues, analysis of the SPR data provides a range of relative permittivities for the untreated films from which we estimate $\varepsilon_r = 2.1$ and $\varepsilon_i = 0.0$ for the protonated form, which is transparent at the excitatory wavelength of 632.8 nm, and $\varepsilon_r = 3.0$ and $\varepsilon_i = 1.0$ for the highly coloured merocyanine form (Fig. 9). The studies indicate that the values are independent of the deposition pressure whereas the thickness increases from 0.6 to to 1.5 nm as π alters from 5 to 35 mN m^{-1}.

The protonated films are suitable as ammonia sensors with

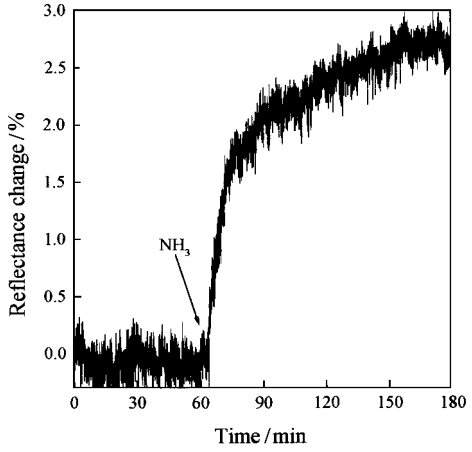

Fig. 10 Variation of the reflectance from the glass–Au–monolayer structure of the protonated form of **1a**, deposited at 15 mN m^{-1}, when exposed to 10 ppm NH_3 in nitrogen at $-0.4°$ from the resonant angle. The percentage change is dependent upon the angle of incidence of the laser beam but is approximately linear with the concentration of gas and the device has a detection limit of *ca.* 1 ppm. Reversal occurs when exposed to an acidified carrier gas.

the concentration monitored by utilising changes in the SPR reflectance at a fixed angle of incidence. The merocyanine and protonated forms are respectively absorbing and transparent at the red end of the spectrum and the large difference in their refractive indices (*e.g.* $\Delta n \approx 0.3$ at 632.8 nm) renders the SPR device sensitive for detection with inexpensive laser diodes. This difference may be compared with the less favourable value of $\Delta n \approx 0.13$ for films of the pyridinium analogue (**2a**), which has a blue-shifted peak absorbance at 510 nm (*cf.* 580 nm for **1a**). The sensitivity of the pyridinium dye may be improved by interrogating at lower wavelengths whereas, from this work, the protonated form of **1a** has a detection limit of *ca.* 1 ppm NH_3 in nitrogen at 632.8 nm (see legend to Fig. 10).

The dyes rapidly switch between the protonated and merocyanine forms in solution. However, when deposited as monolayers on gold-coated glass, the phenolate group is adjacent to the substrate and the time to *ca.* 70% equilibrium is typically 2 to 20 min, this being dependent upon film quality and the difficulty of diffusion in nonporous films. The SPR response is also affected by the ammonium salt, which becomes trapped and results in the film becoming cloudy after a few cycles. However, both problems may be eliminated by self-assembling thiol derivatives of the dyes on the gold surface of the SPR device to ensure that the head group, rather than the alkyl tail, is facing outwards. Current work at Cranfield now involves the synthesis and characterisation of such molecules and their improved behaviour will be reported in a subsequent publication.

Conclusions

The merocyanines form dimeric aggregates in less polar solvents and the chromophores probably adopt a centric antiparallel arrangement in which the molecular dipoles are cancelled. However, the occurrence of SHG, albeit weak, from LB structures of these dyes indicates that the film is non-centrosymmetric. In such films, the quinolinium analogue (**1a**) is tilted towards the substrate with a monolayer thickness of 0.6 to 1.5 nm when deposited at $5 \leqslant \pi \leqslant 35$ mN m^{-1} whereas the pyridinium analogue (**2a**) is tilted towards the vertical with a thickness of 2.2 ± 0.3 nm for $\pi \geqslant 20$ mN m^{-1}. The dyes may be used as sensors for ammonia but, at wavelengths of the inexpensive laser diodes, the quinolinium analogue is more appropriate because its different forms are strongly absorbing (merocyanine) and transparent (protonated). This optimises the refractive index change and, therefore, the response from the SPR device.

Acknowledgements

One of us (G.J.A.) is grateful to the EPSRC UK for funding this work and for providing studentships to K.S. and G.A.N.P.

References

1 G. J. Ashwell, *J. Mater. Chem.*, 1999, **9**, 1991 (Feature Article).
2 C. Bosshard, K. Sutter, P. Prêtre, J. Hulliger, M. Flörsheimer, P. Kaatz and P. Günter in *Organic Nonlinear Optical Materials, Advances in Optics*, Vol. 1, eds. A. F. Garito and F. Kajzar, Gordon and Breach, Basel, 1995.
3 F. Würthner and S. Yao, *Angew Chem., Int. Ed.*, 2000, **39**, 1978.
4 G. J. Ashwell, G. Jefferies, E. J. C. Dawnay, A. P. Kuczynski, D. E. Lynch, G. Yu and D. G. Bucknall, *J. Mater. Chem.*, 1995, **5**, 975.
5 G. J. Ashwell, G. J. Ashwell, J. R. Sambles, A. S. Martin, W. G. Parker and M. Szablewski, *J. Chem. Soc., Chem. Commun.*, 1990, 1374; A. S. Martin, J. R. Sambles and G. J. Ashwell, *Phys. Rev. Lett.*, 1993, **70**, 218.
6 R. M. Metzger, B. Chen, U. Hopfner, M. V. Lakshmikantham, D. Vuillaume, T. Kawai, X. Wu, H. Tachibana, T. V. Hughes, H. Sakurai, J. W. Baldwin, C. Hosch, M. P. Cava, L. Brehmer and G. J. Ashwell, *J. Am. Chem. Soc.*, 1997, **119**, 10455.

7 G. J. Ashwell, E. J. C. Dawnay, A. P. Kuczynski, M. Szablewski, I. M. Sandy, M. R. Bryce, A. M. Grainger and M. Hasan, *J. Chem. Soc., Faraday Trans. II*, 1990, **86**, 1117.
8 J. W. Baldwin, B. Chen, S. C. Street, V. V. Konovalov, H. Sakurai, T. V. Hughes, C. S. Simpson, M. V. Lakshmikantham, M. P. Cava, L. D. Kispert and R. M. Metzger, *J. Phys. Chem.*, 1999, **103**, 4269.
9 S. Rajagopal and E. Buncel, *Dyes Pigm.*, 1991, **17**, 303.
10 S. Arai, H. Arai, M. Hida and T. Yamagishi, *Heterocycles*, 1994, **38**, 2449.
11 C. Machado, M. de G. Nascimento and M. C. Rezende, *J. Chem. Soc., Perkin Trans. 2*, 1994, 2539; L. Dasilva, C. Machado and M. C. Rezende, *J. Chem. Soc. Perkin Trans. 2*, 1995, 483.
12 D. W. Allen and X. Li, *J. Chem. Soc. Perkin Trans. 2*, 1997, 1099.
13 C. Reichardt, S. Lobbecke, A. M. Mehranpour and G. Schafer, *Can. J. Chem.*, 1998, **76**, 686.
14 G. J. Ashwell, K. Skjonnemand, M. P. R. Roberts, D. W. Allen, X. Li, J. Sworakowski, A. Chyla and M. Bienkowski, *J. Colloids Surf.*, 1999, **155**, 43.
15 E. Hamman and A. M. El-Nahas, *J. Phys. Chem. A*, 1998, **102**, 9739.
16 S. F. Alberti and J. Echave, *Chem. Phys.*, 1997, **223**, 183.
17 J. Catalan, E. Mena, W. Meutermans and J. Elguero, *J. Phys. Chem.*, 1992, **96**, 3615.
18 C. Reichardt, *Solvents and Solvent Effects in Organic Chemistry*, 2nd edn., VCH, Weinheim, 1988.
19 H. A. Benesi and J. H. Hildebrand, *J. Am. Chem. Soc.*, 1949, **71**, 2703.
20 D. Flannery, S. W. James, R. P. Tatam, G. J. Ashwell, D. W. Allen and X. Li, *Proc. SPIE – Int. Soc. Opt. Eng.*, 1997, **3105**, 144.
21 E. Kretschmann, *Z. Phys.*, 1971, **241**, 313.
22 G. Sauerbrey, *Z. Phys.*, 1959, **155**, 206.
23 G. J. Ashwell, M. P. S. Roberts, N. D. Rees, G. S. Bahra and C. R Brown, *Langmuir*, 1998, **14**, 5279.